Uncertainty in measuring laminar burning velocity from expanding methane-air flames at low pressures

Pierre Brequigny, H Uesaka, Z Sliti, D Segawa, Fabrice Foucher, Guillaume Dayma, Christine Mounaïm-Rousselle

Uncertainty in measuring laminar burning velocity from expanding methane-air flames at low pressures

P. Brequigny*, H. Uesaka**, Z. Sliti*, D. Segawa**, F. Foucher*,G. Dayma***, C. Mounaïm-Rousselle*
pierre.brequigny@univ-orleans.fr
* Univ. Orléans, INSA-CVL, PRISME, EA 4229, F45072, Orléans, France
** Department of Mechanical Engineering, Osaka Prefecture University, Japan
*** CNRS-INSIS, Institut de Combustion, Aérothermique, Réactivité et Environnement, F45071, Orléans, France

Abstract
The experimental determination of laminar burning velocity remains essential to evaluate the combustion potential of any fuels but also to validate kinetic mechanisms. Recently, researchers are making great efforts to improve the accuracy of the different set-ups and techniques to determine this parameter. This work proposes an attempt to summarize the different factors contributing to the uncertainty of the expanding spherical flame method. In particular, the validity of two hypothesis (adiabatic flame propagation and thin flame front) is discussed in the case of stoichiometric methane-air flames in low-pressure environment (from 0.2 to 2 bar). Last, the effect of spark electrode diameters was also considered (0.2, 0.5 and 1 mm).
Keywords: LF, laminar flame speed, methane, spherical propagation, uncertainty

Introduction

The unstretched Laminar Burning Velocity (LBV) is the one of main properties to evaluate combustion process as in the case of spark-ignition engines, to predict the burning rate. Moreover, accurate measurements of the unstretched LBV remain necessary to improve kinetics model but also to provide correlations for CFD purpose especially for complex fuels or fuel blends.
The experimental estimate of unstretched LBV can be done following different techniques [1] and flame set-ups as Bunsen flame [2,3], counter-flow flame [4,5], flat flame burner [6,7], or outwardly expanding spherical flame with optical diagnostics [8,9] or measurement techniques (heat flux [6,7], pressure signal [10,11]). Since the 1980's the scatters in LBV measurements decrease a lot thanks to the formulation of the stretched flame theory [12]. In the case of outwardly expanding and counter-flow flames, initially the unstretched LBV was obtained from the following linear equation [13]:

$$S_b^0 = S_b - L_b K \quad (1)$$

With S_b^0 the unstretched flame speed related to the burnt gases, S_b the stretched flame speed, L_b the Markstein length representing the mixture stretch sensitivity and K the flame stretch. The unstretched laminar burning velocity, S_L^0 is then obtainedby:

$$S_L^0 = \frac{\rho_b}{\rho_u} * S_b^0 \quad (2)$$

With ρ_b and ρ_u respectively the burnt and unburnt gas density.
More recently, Kelley and Law [14] proposed a Non-Linear Extrapolation (NLE) based on the theoretical work of Tien and Matalon [15] and applied to the outwardly spherical flame technique [16] as follows:

$$\left(\frac{S_b}{S_b^0}\right)^2 \ln\left(\frac{S_b}{S_b^0}\right) = -\frac{2L_b K}{S_b^0} \quad (3)$$

Recently, several authors tested a wide range of different extrapolation methods for the outwardly spherical expanding flames [17,18] in order to quantify the uncertainties generated by the extrapolation method. These studies mainly concluded that as function of the fuel/mixture properties, especially the Lewis number, the extrapolation method has to be

carefully chosen. Wu et al. [18] concluded that if the controlling parameter defined as the Markstein number, obtained from linear extrapolation multiplied by the normalized stretch value at middle point of the data, is in the range of -0.05 to 0.15, any extrapolation method can be used. On the other hand, Li et al. [17] proposed a new NLE for Lewis number greater or close to unity. They also showed that the choice of the extrapolation method would affect differently the estimate of the unstretched LBV, depending on the flame radius range used for the extrapolation.

Studies regarding the uncertainty quantifications caused by the experimental set-up and data processing are quite sparse. Recently Beeckmann et al. [19] did a collaborative study on different experimental set-ups to understand the origin of the discrepancies. They showed that LBV values of stoichiometric methane-air mixtures at 1 bar, 300 K obtained from heat flux burner and counter-flow flames are slightly higher than for the spherical vessel except when LBV is obtained from the fresh gases [9]. Alekseev et al. [7] recently studied in depth the uncertainties to determine LBV with the heat flux burner technique: more than 20 sources of uncertainties were identified. Some of them are specific to this technique itself but others can be considered for any techniques (as fuel purity, air composition, mass flow controllers, mixing process, initial mixture temperature and pressure control, flame surface area …). Until now, no studies dedicated to the uncertainty quantification for the outwardly spherical expanding flame technique can be found in the literature. Therefore, the objective of this work is to study the uncertainty origins to display experimental data with relevant uncertainty values. This paper will also highlight the difficulty of measuring accurately LBV at low pressure due to the thin flame hypothesis and the spark electrode effect. The uncertainties will be estimated in the case of stoichiometric methane/air mixture for different initial pressures (from 0.2 to 2 bar) at an initial temperature of 298 K.

Experimental setup

Experiments were carried out in a spherical stainless steel combustion chamber with an inner volume of 4.2 L (inner diameter 200 mm) fully described by Galmiche et al. [20]. A heater wire resistance located on the outer surface of the sphere maintains the initial gases temperature at chosen value. The device is equipped with a vacuum pump to achieve a residual pressure lower than 0.003 bar before fill the chamber. The volumes of synthetic air (79.1% N_2 and 20.9% O_2 vol.) and pure CH4 (99.99%) were introduced thanks to thermal flowmeters (Brooks 5850S, 2 NL/min for air, and 0.5 NL/min for methane). One fan is used to mix homogenously the gases and stopped 5s before ignition to avoid any perturbation during the flame propagation experiments. A piezoelectric pressure transducer and a K-type thermocouple are used to check the pressure level and the initial temperature before ignition. Two tungsten electrodes, with a 1-mm gap, linked to a conventional capacitive discharge ignition system generate a spark at the center of the chamber. Three electrodes diameters were tested: 0.2, 0.5 and 1 mm. The duration of coil charge for ignition was fixed at 3ms, to ensure a similar ignition energy.

The flame propagation was visualized using a double Schlieren view method through two opposite and transparent pairs of windows (diameter 70 mm) installed on the chamber. A scheme of the set-up is presented in Fig.1. Both, side and front views are recorded by the high-speed camera (Phantom v1610) thanks to a prism assembly at 10000 images per second, with 0.1025 mm/pixel magnification ratio and a resolution of 640x800 pixels² for each view. The double Schlieren set-up enables to visualize the flame propagation in both directions mainly to observe the impact of electrodes on the flame sphericity: as it can be seen in Table 1.

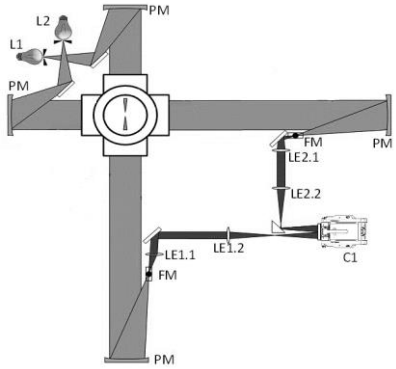

Figure 1. Schematic overview of the set-up. L1,L2 : LED lamps ; PM: Parabolic mirror (864 mm focal length); FM: Focal metric; LE: Lenses (focal length: 200 mm and 160 mm respectively).

The instantaneous flame front radius, $R_f$was obtained from image processing and the laminar flame speed S_b from its temporal derivative, as $S_b = dR_\mathrm{f}/\mathrm{d}t$. By using Eq.3, i.e. NLE, the unstretched laminar flame propagation velocity S_b^0 is deduced, as the use of this nonlinear equation yields better results mainly under fuel-lean conditions, where the Markstein length from burnt gases side reaches or exceeds 1 mm [16]. For spherically expanding laminar flames, the total stretch K acting on the flame is equal to $2 * S_b/R_f$. ρ_u and ρ_b needed to determine S_L^0, from Eq. (2) were computed using the EQUIL code from the CHEMKIN package[21].

Table 1. Example of flame evolution from front and side view images for different electrode diameters. (stoichiometric CH4-air, 0.5 bar, 298 K).

Electrode diameter	1 mm	0.5 mm	0.2 mm
Front view (15 ms after spark)	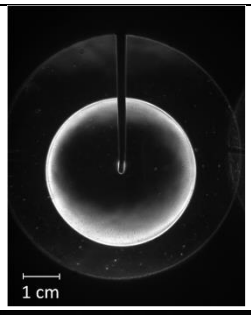	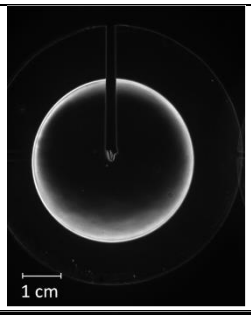	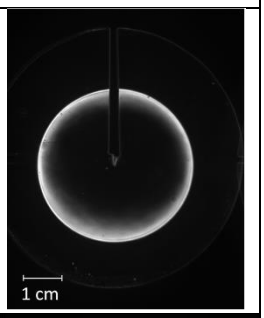
Side view (10 ms after spark)	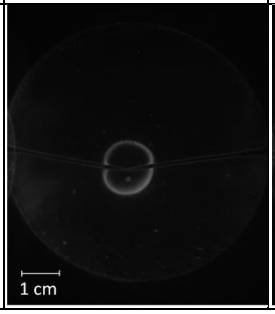	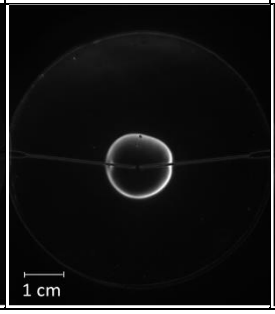	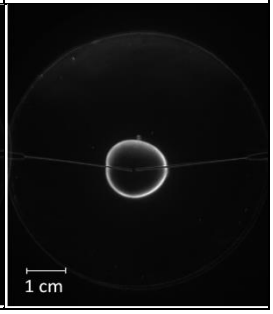

Side view (15 ms after spark)	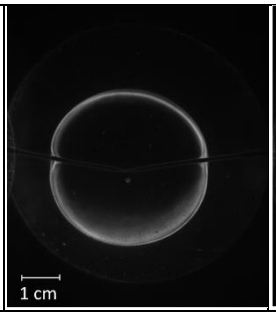	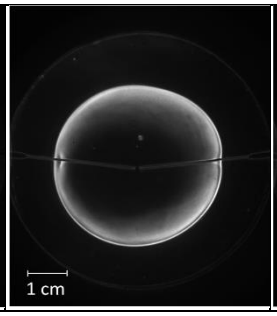	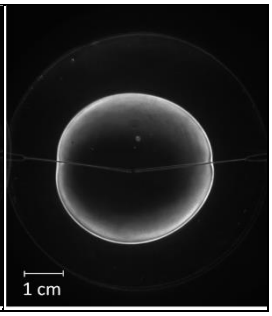

Experimental errors and uncertainty quantification

As the purpose here is to identify all sources of experimental errors in order to suggest a method as described by Moffat [22], based on the combination of experimental and statistical errors detailed in Table 2. The global uncertainty (or 'bias'), $B_{S_L^0}$ can be calculated as Eq. 4,

$$B_{S_L^0} = \sqrt{\left(\frac{\Delta S_L^0}{S_L^0}\right)^2_{P,T,\nu_{O_2}} + \left(\frac{\Delta S_L^0}{S_L^0}\right)^2_{imaging} + \left(\frac{\Delta S_L^0}{S_L^0}\right)^2_{statistical}} \quad (4)$$

Table 2. Names and origins of the errors

Formula	Name	Origin of errors
$\left(\frac{\Delta S_L^0}{S_L^0}\right)_{P,T,\nu_{O_2}}$	Experimental hardware errors	control of the initial conditions
$\left(\frac{\Delta S_L^0}{S_L^0}\right)_{imaging}$	Imaging errors	the imaging technique and processing
$\left(\frac{\Delta S_L^0}{S_L^0}\right)^2_{statistical}$	Statistical error	evaluated by running several identical tests

Experimental hardware errors

From Eq. 5 (Metghalchi and Keck's correlation [10]), this experimental error due to the accuracy of the initial conditions (as P, pressure, T, temperature and ν_{O_2}, oxygen rate) can be deduced as Eq.6 (subscript ref = reference conditions) :

$$S_L^0 = S_{L,ref}^0 \left(\frac{T}{T_{ref}}\right)^{\alpha} \left(\frac{P}{P_{ref}}\right)^{\beta} \left(\frac{\nu_{O_2}}{\nu_{O_{2,ref}}}\right)^{\gamma} \quad (5)$$

$$\left(\frac{\Delta S_L^0}{S_L^0}\right)_{P,T,\nu_{O_2}} = |\alpha|\frac{\Delta T}{T} + |\beta|\frac{\Delta P}{P} + |\gamma|\frac{\Delta \nu_{O_2}}{\nu_{O_2}} \quad (6)$$

As the coefficients $\alpha, \beta,$ and γ depend on the equivalence ratio, to evaluate the errors, the 'worst' values have to be considered for those coefficients. From previous studies [23], the coefficients α, β, γ were determined as respectively 1.89, -0.41, 2.67. The Relative errors for the initial pressure, temperature and oxygen from the present set-up are respectively 1, 0.7 and 0.6% and induce a global experimental hardware error of 1.2%.

Imaging errors

Another cause of experimental errors is due to the set-up of the camera itself (i.e. frame speed and size). Beeckmann et al. [19] showed that the relative errors generated by the resolution on the flame speed are below 1.5 %. Moreover, another error due to the image processing to detect flame contour has also to be considered. For that, as the smallest flame circle can contain a 2x2 pixels² square, when detecting the contour, the maximum detection error corresponds to the largest distance in a pixel, i.e. the diagonal. Therefore, the detection error on the radius, ΔR_f is $\sqrt{2}$ pixel. Two minimum and maximum radii are then defined as follows:

$R_{f,min} = R_f - \Delta R$ and $R_{f,max} = R_f + \Delta R$ (7)

The flame speed and stretch can be calculated from the evolution of $R_f, R_{f,min}$ and $R_{f,max}$ and NLE (Eq. 3) applied for those 3 evolutions to provide 3 values of unstretched laminar flame speed $S_b^0, S_{b,-}^0$and $S_{b,+}^0$ respectively. This uncertainty on R_f is then $\max\left(\frac{|S_b^0-S_{b,-}^0|}{S_b^0}; \frac{|S_b^0-S_{b,+}^0|}{S_b^0}\right)$. For experimental set-up here, this estimate leads to 1% error, and thus a global imaging error of 2.5 % is estimated by adding the 1.5% implied by the resolution error described previously.

Statistical error

As discussed previously, the statistical error needs to be calculated not only to check the repeatability of the measurement but also to include it in the uncertainty calculation of Eq. 4. From several tests done for the same experimental conditions, the mean value is first calculated as follows: $\bar{x} = \frac{1}{n}\sum_{i=1}^{n} X_i$, with n the number of tests and X_i, the value of the test numbered i. The standard deviation is obtained as usual $\sigma_x = \sqrt{\frac{1}{n}\sum_{i=1}^{n}(X_i - \bar{x}\,)^2}$.

The interval of confidence is then given using the Student's law as follows:

$$\bar{x} - t\frac{\sigma_x}{\sqrt{n}} \leq \bar{x} \leq \bar{x} + t\frac{\sigma_x}{\sqrt{n}} \quad (8)$$

with t the value of the Student's density function.

With the determination of t from Student's table, the statistical error is then obtained and included in the global uncertainty estimate through Eq.4. The method described here will be applied to the following results obtained for stoichiometric methane-air combustion at sub-atmospheric pressures.

Results and discussion

When the unstretched laminar burning speed is determined from spherical expanding flame, several hypothesis are done [9]. Among them, the adiabatic flame as well as the thin flame are of importance. The flame speed measurement has to be done when the flame is far from the walls of the vessel to avoid heat losses effect and consider the adiabatic flame hypothesis, but also to consider the constant pressure during the flame expansion. In this study, it was limited to for flame diameters below 50 mm, corresponding to a burnt gases volume less than 1.6% of the chamber volume. In the other hand, the effects of the ignition and electrodes themselves have to be also avoid, thereafter only images corresponding to a flame front radius greater than 6.5 mm were used [24]. In the case of sub-atmospheric flames, heat losses with electrodes in comparison to the flame energy could be critical, moreover as the flame is thickened, the flame speed estimate from the flame front radius evolution based on thin flame thickness can be less accurate. To study these both effects in the case of sub-atmospheric environment, stoichiometric methane-air mixture was chosen to avoid thermo-diffusive instability and 3 different diameters of tungsten electrodes (namely 0.2, 0.5 and 1.0 mm) to evaluate the impact of heat loss through the electrodes. At fixed initial temperature (298 K), experiments were carried out for 8 different initial pressures (0.2, 0.3, 0.4, 0.5, 0.6, 0.8, 1.0, and 2.0 bar). For all experiments presented in following, the results are the average of 3 experiments and the error bars corresponding to the global uncertainty bias, $B_{S_L^0}$ calculated from Eq.4.

Electrodes effect

Fig. 2 displays the laminar burning speed as a function of pressure for the three different sizes of electrodes in comparison with the previous work of Konnov et al. [25]. It can be seen that for pressures equal to 1 and 2 bar, the results obtained with any electrode diameter are in a good agreement with the data provided by Konnov et al. The variations for different electrode diameters, lower than 1 cm/s are in the range of the uncertainty. But for sub-atmospheric initial pressure, the difference between the data of Konnov et al. obtained with heat flux burner increase as a function of pressure decrease. Moreover, until 0.4 bar, the difference between 0.5 and 1 mm diameter is really low but below 0.4 bar, the flame was ignited only for the two lower

electrode diameters, due to the too strong heat losses towards the electrodes compared to the flame energy whereas the 0.5 mm electrodes enabled to ignite mixture down to 0.2 bar.

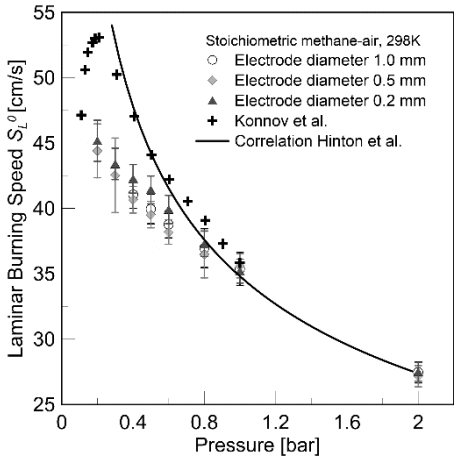

Figure 2. Laminar Burning speed as a function of pressure for 3 electrode diameters and from Konnov et al. [25].

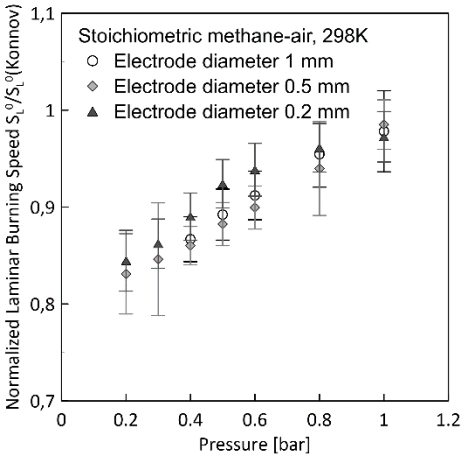

Figure 3. Normalized Flame Speed S_L^0/S_L^0 (Konnov) versus pressure.

In order to highlight the differences with the data of Konnov et al., our LBV values were normalized by Konnov et al values as displayed in Fig. 3. It can be seen that at 1 bar, the results obtained with all the electrodes are really similar to those of Konnov et al. As the pressure decreases, the normalized flame speed decreases down to 0.83 (in the case of 0.5 mm electrode diameter). The use of 0.5 mm electrodes instead of 1 mm electrodes is less impacting on flame speed values but it enables to ignite at lower pressure. However, when using the 0.2 mm electrodes, the normalize flame speed is slightly increased and the uncertainty decreases due to a lower standard deviation thus improving the quality of the results. Nevertheless, taking into account the uncertainty does not allow to values similar to what Konnov et al. measured at low-pressure. Other values from literature can be extracted: at 0.167 (Ombrello et al. [26]) and 0.25 bar (Egolfopoulos et al. [4]) providing LBV of 57.01 and 61.25 cm/s respectively which is even higher than the results of Konnov et al. For the sake of comparison, the correlation proposed by Hinton et al. [27] is presented. This correlation was validated using experimental data covering a range of pressure from 0.25 to 20 bar and more precisely at low pressure with the data of Hassan et al. [28] at 0.25 and 0.5 bar and Taylor [29] at 0.5 bar. The correlation shows a good agreement with the present dataset down to 0.8 bar. From 0.6 bar, the correlation agrees better with the data of Konnov et al. However it seems that below 0.2 bar, the correlation overestimates the LBV compared to the experimental values of Konnov et al.

Thanks to the double Schlieren set-up described in Fig. 1, the heat losses toward the electrodes can be observed for both views as in Table 1. From the front view, 15 ms after the Start of Spark Ignition (SSI), no effect on electrode diameter can be identified on the flame shape but from the side view, the effect of the electrodes is clearly visible especially earlier, i.e 10 ms after SSI. Indeed, for the 1 mm electrodes, the flame, affected by electrodes heat losses, looks like a combination of 2 half circles whereas for smaller electrodes the flame shape is more continuously circular. The deformation of the flame shape is not distinguishable with the decrease of electrode diameter especially as a function of the flame growth (as 15 ms after SSI and a flame diameter around 40 mm). The deformation corresponding to the heat losses from the flame kernel towards the electrodes induces a non-homogeneous local flame speed altering the accuracy of the burning speed estimate from this technique. It is then clearly demonstrated that as a function of the initial pressure, the ignition device characteristics have to be taken into account to consider discrepancies of flame speed data from literature.

Taylor [29] showed that as a function of electrodes size, the minimum radius considered for the extrapolation should be adjusted due to a "volumetric error" linked to the heat loss towards the electrodes. The flame radius will increase quicker than expected because the electrodes occupy a part of the burnt gas volume. It is clear that this influence becomes negligible as the flame grows. The magnitude of the volumetric error can be estimated by representing the electrodes by a single rod passing through the center of the flame. The ratio of rod volume to flame volume is $1.5\left(R_{electrodes}/R_f\right)^2$ with $R_{electrodes}$ the radius of the electrodes. To discount the electrode effects the above ratio should be lower than 0.01 according to Taylor. As a consequence, the minimum flame radius that must be considered in the present work is 6.1 mm, 3 mm and 1.2 mm for electrode diameter of 1, 0.5 and 0.2 mm respectively. Since the minimum radius chosen for the extrapolation is 6.5 mm that implies that, the effect of the electrodes could be neglected.

Flame thickness hypothesis

Taking into account the flame thickness in the experimental determination of LBV is a quite old issue [30]. Recently Liang et al. [31] proposed a new extrapolation expression based on the work of Frankel and Sivashinsky[32] and Chen and Ju[33] to take into account the flame thickness. From the asymptotic solution allowing the finite flame thickness developed by Frankel and Sivashinsky, Chen and Ju presented this expression

$$\left(U+\frac{2}{R}\right)\ln\left(U+\frac{2}{R}\right)=\frac{(Z-2)}{R}\left(\frac{1}{Le}-1\right) \quad (9)$$

with U, R, Le, and Z respectively the normalized flame speed, the normalized flame radius, the Lewis Number and the Zel'dovich number. Therefore this equation can be written in a dimensional form called "Flame Thickness Expression" (FTE) as :

$$\left(\frac{S_b}{S_b^0}+\frac{\delta_L^0}{R_f}\right)\ln\left(\frac{S_b}{S_b^0}+\frac{\delta_L^0}{R_f}\right)=-\frac{2(L_b-\delta_L^0)}{R_f} \quad (10)$$

with δ_L^0, the flame thickness. This expression is similar to the nonlinear extrapolation of Eq. 3 and in the limit of a very thin flame the term corresponding to the flame thickness in Eq. 10 vanishes. However, as δ_L^0 increases with the pressure decrease, the thin flame hypothesis becomes less and less valid for the burning speed measurement using the spherical expanding flame technique. A new post-process based on this new expression was done to quantify this effect of the flame thickness on LBV estimate at low pressure. To evaluate the impact of δ_L^0 on S_b^0 experimental estimate, the flame thickness value was arbitrary varied from 0 to 0.5 cm as presented in Fig. 4 for an initial pressure of 0.2 bar. A variation of the flame thickness from 0 to 0.5 cm modifies the unstretched flame speed value up to 11 cm/s thus leading to a difference of 3.25 %, on the unstretched LBV. It can be noted that S_b^0 estimate reaches a maximum value for a flame thickness of 0.16 cm which corresponds to the theoretical flame thickness calculated for those conditions by using the classical expression $T_{ad}-T_u/\max(dT/dx)$ with GRI-Mech 3.0 [34] as indicated Table 2.

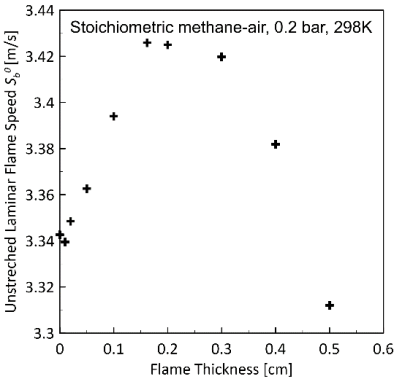

Figure 4. Unstretched laminar flame speed as a function of arbitrary flame thickness value.

The comparison between the two extrapolation methods, namely NLE (Eq. 3) and FTE (Eq. 10) by taking the δ_L^0 estimate is then presented in Table 3 for 4 pressures values and an electrode diameter of 0.2 mm. It can be noted that FTE method provides higher LBV values than NLE method. However, this increase is not sufficiently important to reach Konnov et al. values. As a conclusion, by taking into account the flame thickness and by using the thinnest electrodes appear to be not sufficient to fill the gap between the present data and those of Konnov et al. or also those predicted by GRI-Mech 3.0 (given in Table 3), 5% lower than Konnov et al. measurements.

Table 3. Comparison of different laminar burning speed estimates and flame thickness versus pressure. Stoichiometric methane-air, 298K.

Pressure (bar)	Flame Thickness from GRi 3.0 (mm)	LBV from GRI 3.0 (cm/s)	LBV Konnov et al. (cm/s)	LBV Present Work NLE (cm/s)	LBV Present Work FTE (cm/s)
0.2	1.62	56.70	53.07	45.18 ± 1.43	46.08 ± 1.65
0.3	1.17	52.39	50.06	43.40 ± 0.97	44.02 ± 1.00
0.4	0.926	49.11	47.30	42.26 ± 0.83	42.58 ± 0.98
0.5	0.773	46.45	44.80	41.42 ± 0.86	41.27 ± 0.81

As a result, the experimental setup and methods used seem to present some limitations to determine with high accuracy unstretched laminar burning speed in such conditions, either the flame thickness is not properly taken into account or other hypothesis used in flame speed measurement need to be investigated. Indeed, as the pressure decreases, the flame thickness increases thus affecting the flame temperature profile. Varea et al.[9] showed on normalized temperature profiles calculated from PREMIX that the distance to reach the equilibrium state increases as decreases the initial pressure. For pressure set investigated in the present study, the temperature profiles normalized by the equilibrium temperature, calculated with GRI-Mech 3.0 on PREMIX, are reported in Fig. 5.

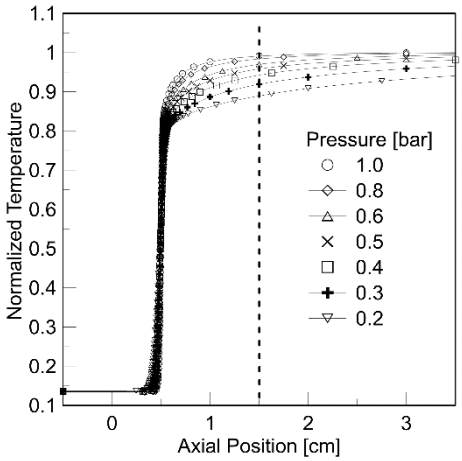

Figure 5. Normalized simulated temperature profiles for stoichiometric methane-air flames at initial temperature of 298 K and various initial pressures.

Fig. 5 shows that at 1 bar, the flame reaches the equilibrium state, identified for 0.99 of normalized temperature at 1.5 cm, whereas at 0.8 bar, it needs 3 cm and 12 cm for the 0.2 bar flame. Therefore, the low-pressure flames investigated in the present study cannot be considered in the equilibrium state, which is one strong hypothesis of the spherical expanding

flame method. This results in an overestimate of the density ratio used in the calculation of S_L^0. The following method is proposed for a first way to estimate what could be the actual density ratio for those low-pressure flames. By considering that at 1 bar, the flame reaches the equilibrium at 1.5 cm, the density ratios of the flame at lower pressure are calculated at the same distance and used for the calculation of S_L^0 like in Eq. 2. The different values of density ratios are reported in Table 4. The relative difference in terms of density ratios between a normalized temperature of 0.99 and the equilibrium is only 1.5 %. The potential change in the laminar burning velocity will be then about 0.5 cm/s and neglected in the case of pressure higher than 0.8 bar.

Table 4. Density ratios estimate for stoichiometric methane-air flames at initial temperatures of 298K.

Pressure [bar]	ρ_b/ρ_u at the equilibrium	ρ_b/ρ_u at X=1.5 cm	Relative difference with the equilibrium [%]
0.8	0.1336	0.1365	2.17
0.6	0.1339	0.1389	3.73
0.5	0.1341	0.1408	5.00
0.4	0.1344	0.1436	6.85
0.3	0.1348	0.1478	9.64
0.2	0.1353	0.1541	13.90

In Fig 6, the effect of correcting the density ratio on the laminar burning velocity measurement by using the values at 1.5 cm as presented in Table 4 is plotted. As expected, the current data present a better agreement with the results of Konnov et al. especially the general trend in the laminar burning speed as a function of pressure is better captured. Moreover by using the FTE model, the data of Konnov et al. are even included in the error bars, except for 0.4 and 0.3 bar. Compared with the results of Table 3, the correction of the density ratios brings improvement with less than 10% of difference with GRI-Mech 3.0 for both NLE and FTE cases and for pressures below 0.4 bar using the FTE extrapolation about 7% of difference as FTE is beneficial when pressure is below 0.4 bar (as seen in Table 3). This demonstrates that a proper estimation of the density ratio is required when dealing with low-pressure flame and its effect is here clearly highlighted.

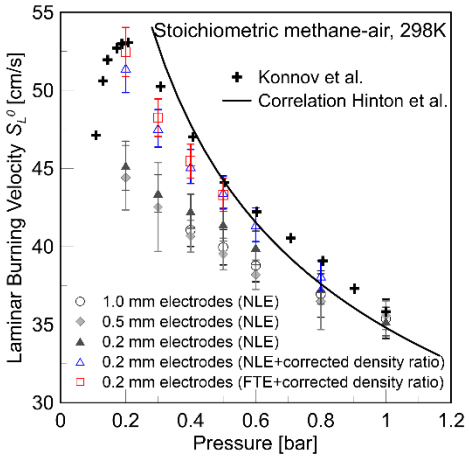

Figure 6. Laminar Burning speed estimate as a function of pressure for 3 electrode diameters, from 2 different extrapolation methods and equilibrium and corrected density ratios.

Conclusion

Accurate measurements of LBV remain of primary importance in order to validate kinetic mechanisms or to provide correlations for CFD modelling especially for complex and/or blend fuels. The objective of this study was to analyze different uncertainties sources in LBV measurements done using the outwardly expanding flame configuration in a closed vessel and to provide rigorous method to estimate them. The method enables to display averaged LBV values together with more realistic error bars corresponding to experimental uncertainties. In the worst case of this study (intake pressure of 0.3 bar with a spark electrode diameter of 0.5mm), the uncertainty was estimated about 6.5%.

The uncertainty method was then applied to sub-atmospheric stoichiometric methane-air premixed flame for which the adiabatic flame and thin flame thickness hypotheses could be invalid. In order to investigate the adiabatic flame hypothesis, different sizes of electrodes were used. Results showed that using electrodes with diameter less than 0.5 mm enables to ignite mixtures at lower pressure and presents higher LBV values for pressure below 0.5 bar, due to the heat losses occurring from the flame towards the surface that lead to a flame distortion and a modification of the flame speed locally. Since the results obtained with the smallest electrode size were still far from those of Konnov et al. [25] or predicted by GRI-Mech 3.0, the flame thickness hypothesis was investigated using the extrapolation method proposed by Liang et al. [31]. Results showed that taking into account the flame thickness in the extrapolation of the unstretched flame speed values has a low impact on the results in the most critical condition (LBV increased by 3.25 % in the best case). Taking into account the flame thickness showed some improvements (1.5 % in the best case) in LBV values but not sufficiently to explain the differebce with Konnov et al. values (up to 20% of difference). Finally, the choice of equilibrium density ratio has been discussed. The simulated flame temperature profiles clearly showed that the equilibrium is probably not reached for sub atmospheric flames and that a proper estimate of the real density ratio for those outwardly expanding flames is required or at least a correction for the density ratio to provide a better estimate of the LBV.

To conclude, the outwardly spherical expanding flame does not seem to be the most accurate technique for measuring LBV at low pressure. The flame thickness is not properly considered or some other hypothesis still need to be improved. For future work, the flame thickness could be considered as an output of the extrapolation method as initially implemented by Liang et al. in order to see how the improvement of result is. Other mixtures, with thin flame thickness even at low pressure could be also investigated in order to verify which parameter is the most impacting in such conditions between the flame thickness and the density ratio.

References

[1] Alexander A. Konnov, Akram Mohammad, Velamati Ratna Kishore, Nam Il Kim, Chockalingam Prathap, Sudarshan Kumar, A comprehensive review of measurements and data analysis of laminar burning velocities for various fuel+air mixtures, Prog. Energy Combust. Sci. 68 (2018) 197–267. doi:10.1016/J.PECS.2018.05.003.

[2] Yi Wu, Vincent Modica, Bjorn Rossow, Frédéric Grisch, Effects of pressure and preheating temperature on the laminar flame speed of methane/air and acetone/air mixtures, Fuel. 185 (2016) 577–588. doi:10.1016/j.fuel.2016.07.110.

[3] Omid Askari, Ziyu Wang, Kevin Vien, Matteo Sirio, Hameed Metghalchi, On the flame stability and laminar burning speeds of syngas/O2/He premixed flame, Fuel. 190 (2017) 90–103. doi:10.1016/j.fuel.2016.11.042.

[4] F.N. Egolfopoulos, P. Cho, C.K. Law, Laminar flame speeds of methane-air mixtures under reduced and elevated pressures, Combust. Flame. 76 (1989) 375–391. doi:10.1016/0010-2180(89)90119-3.

[5] P. S. Veloo, Y. L. Wang, F. N. Egolfopoulos, C. K Westbrook, A comparative experimental and computational study of methanol, ethanol, and n-butanol flames, Combust. Flame. 157 (2010) 1989–2004. doi:10.1016/j.combustflame.2010.04.001.
[6] L P H de Goey, A van Maaren, R M Quax, Stabilization of Adiabatic Premixed Laminar Flames on a Flat Flame Burner, Combust. Sci. Technol. 92 (1993) 201–207. doi:10.1080/00102209308907668.
[7] V. A. Alekseev, J. D. Naucler, M. Christensen, E. J. K. Nilsson, E. N. Volkov, L. P. H. de Goey, A. A. Konnov, Experimental Uncertainties of the Heat Flux Method for Measuring Burning Velocities, Combust. Sci. Technol. 188 (2016) 853–894. doi:10.1080/00102202.2015.1125348.
[8] T. Tahtouh, F. Halter, C. MounaÏm-Rousselle, E. Samson, Experimental Investigation of the Initial Stages of Flame Propagation in a Spark-Ignition Engine: Effects of Fuel, Hydrogen Addition and Nitrogen Dilution, SAE Int. J. Engines. 3 (2010) 1–19. doi:10.4271/2010-01-1451.
[9] E. Varea, V. Modica, A. Vandel, B. Renou, Measurement of laminar burning velocity and Markstein length relative to fresh gases using a new postprocessing procedure: Application to laminar spherical flames for methane, ethanol and isooctane/air mixtures, Combust. Flame. 159 (2012) 577–590. doi:10.1016/j.combustflame.2011.09.002.
[10] M. Metghalchi, J.C. Keck, Burning velocities of mixtures of air with methanol, isooctane, and indolene at high pressure and temperature, Combust. Flame. 48 (1982) 191–210. http://www.sciencedirect.com/science/article/pii/0010218082901274.
[11] A. Omari, L. Tartakovsky, Measurement of the laminar burning velocityusing the confined and unconfined spherical flame methods – A comparative analysis, Combust. Flame. 168 (2016) 127–137. doi:10.1016/j.combustflame.2016.03.012.
[12] Chung K. Law, Combustion at a crossroads: Status and prospects, Proc. Combust. Inst. 31 (2007) 1–29. doi:10.1016/j.proci.2006.08.124.
[13] C.K. Wu, C.K. Law, On the determination of laminar flame speeds from stretched flames, Symp. Combust. 20 (1985) 1941–1949. doi:10.1016/S0082-0784(85)80693-7.
[14] A P Kelley, C K Law, Nonlinear effects in the extraction of laminar flame speeds from expanding spherical flames, Combust. Flame. 156 (2009) 1844–1851. doi:10.1016/j.combustflame.2009.04.004.
[15] J.H. Tien, M. Matalon, On the burning velocity of stretched flames, Combust. Flame. 84 (1991) 238–248. doi:10.1016/0010-2180(91)90003-T.
[16] F Halter, T Tahtouh, C Mounaïm-Rousselle, Nonlinear effects of stretch on the flame front propagation, Combust. Flame. 157 (2010) 1825–1832. doi:10.1016/j.combustflame.2010.05.013.
[17] X. Li, E. Hu, X. Meng, C. Peng, X. Lu, Z. Huang, Effect of Lewis Number on Nonlinear Extrapolation Methods from Expanding Spherical Flames, Combust. Sci. Technol. (2017) 1510–1526. doi:10.1080/00102202.2017.1305369.
[18] F. Wu, W. Liang, Z. Chen, Y. Ju, C. K. Law, Uncertainty in stretch extrapolation of laminar flame speed from expanding spherical flames, Proc. Combust. Inst. 35 (2015) 663–670. doi:10.1016/j.proci.2014.05.065.
[19] J. Beeckmann, N. Chaumeix, P. Dagaut, G. Dayma, F. Foucher, F. Halter, A. Lefebvre, C. Mounaim-Rousselle, H. Pitsch, B. Renou, E. Varea, Collaborative study for accurate measurements of laminar burning velocity, in: Proc. Eur. Combust. Meet. 2013, Lund, Sweden, 2013.
[20] Bénédicte Galmiche, Fabien Halter, Fabrice Foucher, Effects of high pressure, high temperature and dilution on laminar burning velocities and Markstein lengths of iso-octane/air mixtures, Combust. Flame. 159 (2012) 3286–3299.

doi:10.1016/j.combustflame.2012.06.008.
[21] A. E. Lutz, F.M. Rupley, R. J. Kee, EQUIL: A CHEMKIN IMPLEMENTATION OF STANJAN, FOR COMPUTING CHEMICAL EQUILIBRIA, Livermore, 1996.
[22] Robert J. Moffat, Describing the uncertainties in experimental results, Exp. Therm. Fluid Sci. 1 (1988) 3–17. doi:10.1016/0894-1777(88)90043-X.
[23] A.E. Dahoe, L.P.H. de Goey, On the determination of the laminar burning velocity from closed vessel gas explosions, J. Loss Prev. Process Ind. 16 (2003) 457–478. doi:10.1016/S0950-4230(03)00073-1.
[24] D Bradley, R A Hicks, M Lawes, C G W Sheppard, R Woolley, The Measurement of Laminar Burning Velocities and Markstein Numbers for Iso-octane-Air and Iso-octane-n-Heptane-Air Mixtures at Elevated Temperatures and Pressures in an Explosion Bomb, Combust. Flame. 115 (1998) 126–144. doi:10.1016/S0010-2180(97)00349-0.
[25] A.A. Konnov, R. Riemeijer, V.N. Kornilov, L.P.H. de Goey, 2D effects in laminar premixed flames stabilized on a flat flame burner, Exp. Therm. Fluid Sci. 47 (2013) 213–223. doi:10.1016/j.expthermflusci.2013.02.002.
[26] Timothy Ombrello, Campbell Carter, Viswanath Katta, Burner platform for sub-atmospheric pressure flame studies, Combust. Flame. 159 (2012) 2363–2373. doi:10.1016/J.COMBUSTFLAME.2012.03.010.
[27] Nathan Hinton, Richard Stone, Roger Cracknell, Laminar burning velocity measurements in constant volume vessels – Reconciliation of flame front imaging and pressure rise methods, Fuel. 211 (2018) 446–457. doi:10.1016/J.FUEL.2017.09.031.
[28] M I Hassan, K T Aung, G M Faeth, Measured and predicted properties of laminar premixed methane/air flames at various pressures, Combust. Flame. 115 (1998) 539–550. http://www.sciencedirect.com/science/article/pii/S001021809800025X.
[29] Simon Crispin Taylor, Burning velocity and the influence of flame stretch, University of Leeds, 1991.
[30] A.M. Garforth, C.J. Rallis, Laminar burning velocity of stoichiometric methane-air: pressure and temperature dependence, Combust. Flame. 31 (1978) 53–68. doi:10.1016/0010-2180(78)90113-X.
[31] W. Liang, F. Wu, C. K. Law, Extrapolation of laminar flame speeds from stretched flames: Role of finite flame thickness, Proc. Combust. Inst. (2016). doi:10.1016/j.proci.2016.08.074.
[32] M L Frankel, G I Sivashinsky, On Effects Due To Thermal Expansion and Lewis Number in Spherical Flame Propagation, Combust. Sci. Technol. 31 (1983) 131–138. http://www.tandfonline.com/doi/abs/10.1080/00102208308923635.
[33] Z Chen, Y Ju, Theoretical analysis of the evolution from ignition kernel to flame ball and planar flame, Combust. Theory Model. 11 (2007) 427–453. http://dx.doi.org/10.1080/13647830600999850.
[34] G. P. Smith, D. M. Golden, M. Frenklach, N.W. Moriarty, B. Eiteneer, M. Goldenberg, C. T. Bowman, R. K. Hanson, S. Song, W. C. Jr. Gardiner, V. V. Lissianski, Z. Qin, GRI-Mech 3.0, (n.d.). http://www.me.berkeley.edu/gri_mech/.